ARTICLE IN PRESS

Available online at www.sciencedirect.com

SCIENCE DIRECT®

ELSEVIER

EPSL

Earth and Planetary Science Letters xx (2004) xxx–xxx

www.elsevier.com/locate/epsl

Astronomic calibration of the late Oligocene through early Miocene geomagnetic polarity time scale☆

K. Billups[a,*], H. Pälike[b,1], J.E.T. Channell[c], J.C. Zachos[d], N.J. Shackleton[e]

[a] College of Marine Studies, University of Delaware, 700 Pilottown Road, Lewes, DE 19958, USA
[b] Department of Geology and Geochemistry, Stockholm University, S-10691 Stockholm, Sweden
[c] Department of Geological Sciences, University of Florida, PO Box 112120, Gainesville, FL 32611, USA
[d] Department of Earth Sciences, University of California Santa Cruz, Santa Cruz, CA 95064, USA
[e] Godwin Institute for Quaternary Research, University of Cambridge, New Museums Site, Pembroke Street, Cambridge, CB2 3RS, UK

Received 16 October 2003; received in revised form 26 April 2004; accepted 4 May 2004

Abstract

At Ocean Drilling Program (ODP) Site 1090 (subantarctic South Atlantic), benthic foraminiferal stable isotope data (from *Cibicidoides* and *Oridorsalis*) span the late Oligocene through early Miocene (~24–16 Ma) at a temporal resolution of ~5 ky. Over the same interval, a magnetic polarity stratigraphy can be unequivocally correlated to the geomagnetic polarity time scale (GPTS), thereby providing direct correlation of the isotope record to the GPTS. In an initial age model, we use the newly derived age of the Oligocene/Miocene (O/M) boundary of 23.0 Ma of Shackleton et al. [Geology 28 (2000) 447], revised to the new astronomical calculation (La_{2003}) of Laskar et al. [Icarus (in press)] to recalculate the spline ages of Cande and Kent [J. Geophys. Res. 100 (1995) 6093]. We then tune the Site 1090 $\delta^{18}O$ record to obliquity using La_{2003}. In this manner, we are able to refine the ages of polarity chrons C7n through C5Cn.1n. The new age model is consistent, within one obliquity cycle, with previously tuned ages for polarity chrons C7n through C6Bn from Shackleton et al. [Geology 28 447–450 (2000)] when rescaled to La_{2003}. The results from Site 1090 provide independent evidence for the revised age of the Oligocene/Miocene boundary of 23.0 Ma. For early Miocene polarity, chrons C6AAr through C5Cn, our obliquity-scale age model is the first to allow a direct calibration to the GPTS. The new ages are generally within one obliquity cycle of those obtained by rescaling the Cande and Kent [J. Geophys. Res. 100 (1995) 6093] interpolation using the new age of the O/M boundary (23.0 Ma) and the same middle Miocene control point (14.8 Ma) used by Cande and Kent [J. Geophys. Res. 100 (1995) 6093].
© 2004 Published by Elsevier B.V.

Keywords: astrochronology; geomagnetic polarity time scale; oxygen isotopes; late Oligocene; early Miocene

1. Introduction

Shackleton et al. [1,2] established the first astronomical calibration of Oligocene and Miocene time by tuning magnetic susceptibility (lithological) cycles in high-quality deep-sea cores from Ceara Rise, western equatorial Atlantic, to orbital cycles calculated by

☆ Supplementary data associated with this article can be found, in the online version, at doi: 10.1016/j.epsl.2004.05.004.

* Corresponding author. Tel.: +1-302-645-4249; fax: +1-302-645-4007.

E-mail address: kbillups@udel.edu (K. Billups).

[1] Now at Southampton Oceanography Centre, School of Ocean & Earth Science, European Way, Southampton SO14 3ZH, UK.

0012-821X/$ - see front matter © 2004 Published by Elsevier B.V.
doi:10.1016/j.epsl.2004.05.004

UNCORRECTED PROOF

ARTICLE IN PRESS

Laskar et al. [3]. Although this new time scale represents a very important advancement to achieve its full potential, it needs to be correlated to the geomagnetic polarity time scale (GPTS). A first step toward this goal was realized with the successful development of high-resolution stable isotope records from Ceara Rise Sites 929 and 926 [4–7]. These records exhibit pervasive orbital scale cyclicity and a complete record of major isotope events of the early Miocene, as well as many previously unrecognized minor events. The pronounced orbital periodicity in the $\delta^{18}O$ and $\delta^{13}C$ records serves as a means of transferring the orbital calibration to other marine sequences and to the GPTS. The Ceara Rise sediments did not, however, retain a primary magnetization; therefore, no polarity stratigraphy was obtained. High-resolution isotope stratigraphies at sites where the polarity record is well represented are necessary in order to transfer the orbital calibration of stable isotope records to the GPTS.

In the Cande and Kent time scale [8,9], the Oligocene/Miocene (O/M) boundary is the only GPTS calibration point between the middle Miocene (C5Bn at 14.8 Ma) and the Eocene/Oligocene boundary at 33.7 Ma. Shackleton et al. [10] provided an astronomically calibrated age for the onset of C6Cn.2n (the O/M boundary) of 22.9 Ma, which is 0.9 My younger than the age obtained by Cande and Kent [8,9]. This astronomically calibrated age was derived from correlation of orbitally tuned stable isotope records and biostratigraphic datums from Ceara Rise to stable isotope records and biostratigraphic datums at Deep Sea Drilling Project Holes 522 and 522A, for which a high-quality paleomagnetic record exists. In this manner, Shackleton et al. [10] provided revised ages for late Oligocene through earliest Miocene polarity chrons C7n.2n through C6Cn.1n.

Channell et al. [11] used the new age for the O/M boundary of 22.9 Ma and rescaled the ages of Cande and Kent [8,9] to revise the late Eocene to early Miocene GPTS. More recently, a newly revised orbital solution calculated by Laskar et al. [12] (La_{2003}) allows the magnetic polarity stratigraphy of the late Oligocene through earliest Miocene to be further refined yielding an updated age of 23.0 Ma for the onset C6Cn.2n and the O/M boundary. Retuning to the new calculation (La_{2003}) entailed a shift of the order of 100 ky toward older ages. The tuning is well constrained by the 100 ky amplitude modulation of the precession signal in the data, and the solution (La_{2003}), as well as a new solution by Varadi et al. [13], move the sequence of 100 ky eccentricity maxima at around 23 Ma back in time by this amount.

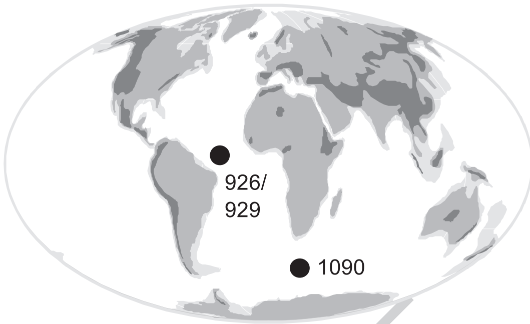

Fig. 1. Location of Leg 177 Site 1090 (43°S, 20°W, 3699 m water depth) in the subantarctic sector of the Southern Ocean and Leg 154 Sites 926 and 929 (4°N, 43°W, 3598 m water depth and 6°N, 44°W, 4361 m water depth, respectively) on Ceara Rise in the western tropical Atlantic.

Here, we present a high-resolution (~5 ky sampling interval) stable isotope record from Ocean Drilling Program (ODP) Leg 177 Site 1090 (Fig. 1). Orbital tuning of the benthic foraminiferal $\delta^{18}O$ record using La_{2003} provides the age model. Site 1090 yielded an apparently complete polarity stratigraphy for the late Oligocene and early Miocene (~24–16 Ma) derived from u-channel measurements [11]. Thus, this site provides the first opportunity to directly calibrate a portion of the GPTS (C7n.1n through C5Cn) to an astronomically tuned stable isotope record.

2. Geochemical methods

Approximately 40 cm^3 of sediment were taken at 5-cm intervals from 160 mcd (1090E-16H-5) to 72 mcd (1090D-8H-1), spanning the late Oligocene (~24.5 Ma) through early Miocene (~16 Ma). On the new time scale, this is equivalent to an average sample spacing of ~5 ky. Processing of Site 1090 sediments followed standard procedures described in detail by Billups et al. [14].

UNCORRECTED PROOF

Stable isotope analyses are conducted using a VG Prism instrument located at the University of Santa Cruz (UCSC), a VG Optima at Harvard University (HU) and a GV Instruments IsoPrime at the University of Delaware (see Table 1 in the EPSL Online Background Dataset[2]). The $\delta^{13}C$ and $\delta^{18}O$ values are calibrated to VPDB via NBS-19 and in-house standards (Cararra Marble). Replicate analyses of standards in the size range of the samples suggest that our overall (i.e., Billups et al. [14] and this study) analytical precision is better than 0.07‰ for $\delta^{13}C$ and 0.08‰ for $\delta^{18}O$ ($n \sim 150$). Based on duplicate analyses ($n = 34$), we note a small offset (0.14 ± 0.23‰) between the oxygen isotope data first generated at UCSC and later at HU [14]. Although the small offset is not statistically significant, we apply a correction of −0.14‰ to the record generated at HU. There are no offsets between the portions of the record generated at Santa Cruz and Delaware ($n \sim 30$).

Due to the scarcity of benthic foraminifera, a high-resolution record can only be constructed by using several species of *Cibicidoides* (*Cibicidoides praemundulus*, *Cibicidoides dickersoni*, *Ceocaenus eocaenus* and *Ceocaenus havanensis*) in addition to *Cibicidoides mundulus* and by combining them with *Oridorsalis umbonatus*. *Oridorsalis* $\delta^{13}C$ values are generally not used for paleoceanographic reconstructions because this genus has an infaunal habitat and $\delta^{13}C$ values do not reflect the $\delta^{13}C$ of dissolved inorganic carbon at the sediment water interface. However, analysis of 95 samples of *Cibicidoides* and *Oridorsalis* from the same intervals justifies a constant correction of *Oridorsalis* $\delta^{18}O$ and $\delta^{13}C$ values to *Cibicidoides* ($\delta^{18}O$ correction: −0.4 ± 0.27 ‰; $\delta^{13}C$ correction: +1.3 ± 0.37 ‰) [14]. The species correction assumes that there are no offsets among *Cibicidoides* used, which was not verifiable due to the lack of sufficient intervals containing two or more species. The $\delta^{18}O$ and $\delta^{13}C$ corrections differ from those obtained by Katz et al. [15] (−0.28‰ and +0.72‰, respectively), but agree better with those of Shackleton et al. [16] (−0.5‰ and +1.0‰; respectively). Differences in offset estimates may reflect the importance of regional water mass properties on regional species offsets.

[2] http://www.elsevier.nl/locate/epsl; mirror site: http://www.elsevier.com/locate/epsl.

3. Late Oligocene to early Miocene stable isotope records

Fig. 2 (top panel) shows the Site 1090 stable isotope records placed on an initial age model derived from the new age for the O/M boundary (23.0 Ma), maintaining an age of 14.8 Ma for C5Bn and recalculating the spline ages of Cande and Kent [8,9]. The stable isotope records display marked high-frequency fluctuations superimposed on long-term trends. There are a few outlying data points, which we remove before tuning the record. The few gaps in the record due to a lack of foraminifera are all shorter than one eccentricity cycle (e.g., < 100 ky) and do not hamper correlation of cycles at the eccentricity scale, which we use as a first step in the tuning process. When compared to the composite Ceara Rise record [7], which has been readjusted to the new orbital solution of Laskar et al. [12] because it is more consistent with geologic data [17], we observe excellent agreement in the longer-term stable isotope variability, as well as in the superimposed higher frequencies, for the period of overlap (Fig. 2b, bottom panel). The good agreement indicates that the recalculated spline ages for Site 1090 based on the GPTS and the new age of the O/M boundary (23.0 Ma) already closely match orbital calculations.

As in Billups et al. [14], the vertical scales are offset to highlight the agreement between the $\delta^{18}O$ records as shown in Fig. 2b (bottom panel). The ~0.5 per mil offset between the two records likely reflects differences in deep-water temperatures between the high-latitude Southern Ocean and the western tropical Atlantic [14]. The $\delta^{13}C$ records show no offset, which suggests that during this interval of time basin-to-basin $\delta^{13}C$ gradients are small, which is perhaps related to an overall low oceanic nutrient content [14].

4. Astrochronology

We start with the initial age model noted above and compare the $\delta^{18}O$ time series to a synthetic orbital target curve constructed from normalized values (less mean and divided by the standard deviation) of eccentricity, tilt and precession (ETP). To enhance eccentricity, which is very weak in insolation curves but strong in our data, we combine the three normalized orbital

UNCORRECTED PROOF

ARTICLE IN PRESS

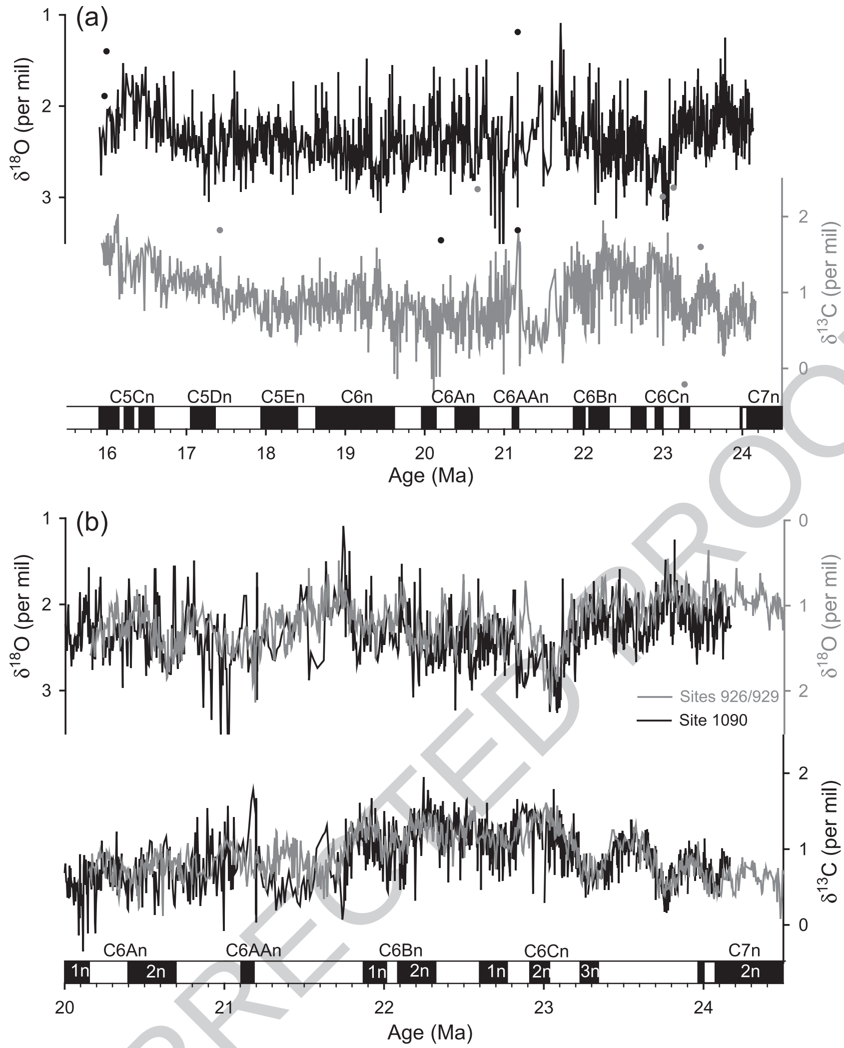

Fig. 2. Site 1090 oxygen and carbon isotope records (top panel, see Table 1 in the EPSL Online Background Dataset[2]) placed on an initial age model derived from the new age of the O/M boundary (23.0 Ma) and recalculated spline ages of Cande and Kent [8,9] (Table 1). Individual data points reflect outliers that we remove before tuning the record. Comparison of Site 1090 stable isotope records in the initial age model to the combined Ceara rise records based on analyses from Sites 926 and 929 [7], which have been retuned using the new orbital solution of Laskar et al. [12] (bottom panel). Late Oligocene through early Miocene polarity chrons with respect to the initial age model for Site 1090 are shown for reference in both panels, and normal polarity chrons are labeled. For a complete list of chron boundaries with respect to the initial age model, refer to Table 1. The recalculated spline ages based on the geomagnetic polarity time scale together with the new age of the O/M boundary (23.0 Ma) applied to Site 1090 are close to tuned ages consistent with astronomical models. Note that two benthic foraminiferal $\delta^{18}O$ records were overlain for comparison purposes. There is a real offset of ~0.5 per mil between the two $\delta^{18}O$ records [14].

components in ratios of approximately 0.3 (E):1 (T):0.2 (P). Following convention, the sign of the $\delta^{18}O$ record is reversed so that minimum $\delta^{18}O$ values are compared with maximum eccentricity values. The ETP-tuned record now provides a framework for further tuning the $\delta^{18}O$ record to obliquity.

For tuning to obliquity, a 7.2 ky time lag is applied to the tilt component of the orbital target. The phase lag arises from retuning of magnetic susceptibility data from Ceara Rise to La_{2003} that was performed by aligning data and target at the climatic precession frequency, constrained by the ~100 ky amplitude

UNCORRECTED PROOF

modulation of precession by eccentricity. This assumption of a zero phase difference at the precession frequency between astronomical solution and geological data results in a phase lag at the obliquity frequency of ~7.2 ky during the late Oligocene. A subsequent iteration applied this phase lag at the obliquity frequency for the calculated ETP curve, generating the overall best-fitting target curve [17]. The zero-phase assumption at precession based on the Ceara Rise records stems from the evidence that the strong precession

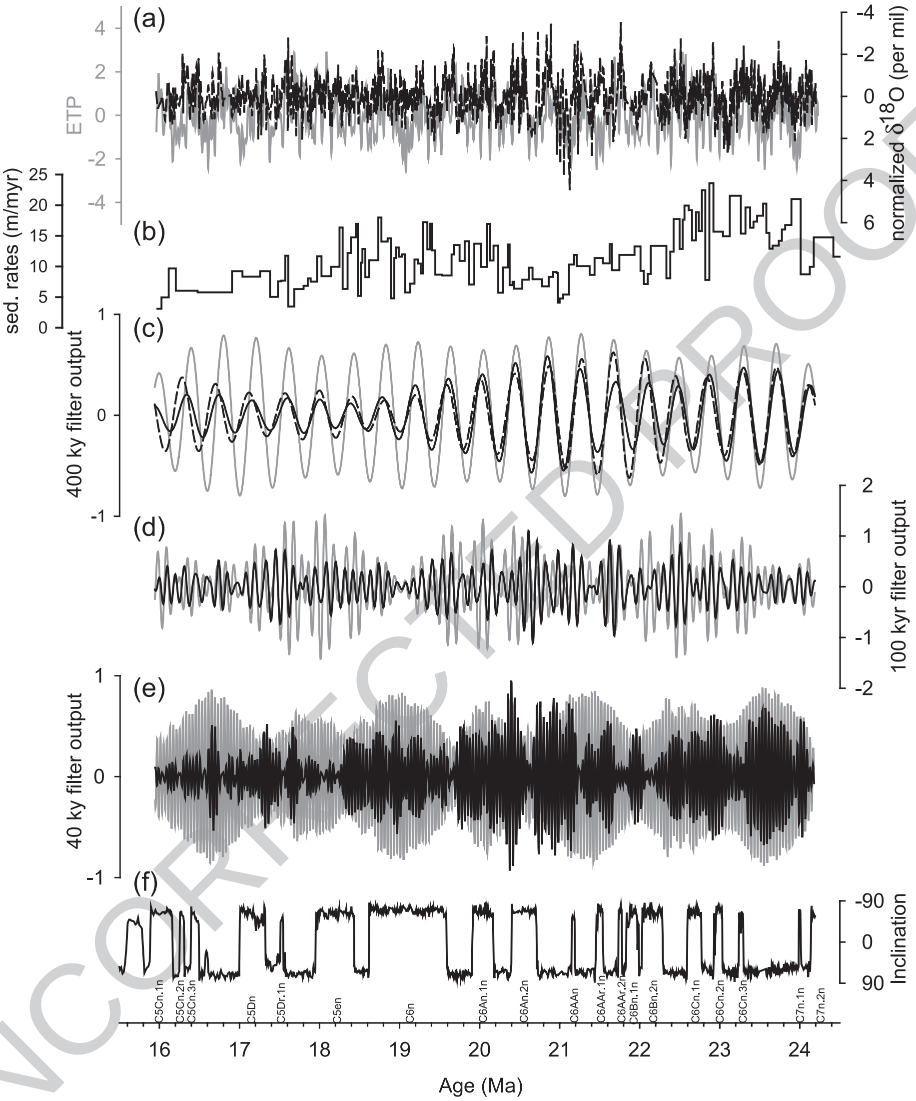

Fig. 3. Summary of tuning results to obliquity scale of the Site 1090 benthic foraminiferal δ^{18}O record. Panel a illustrates a comparison of the normalized δ^{18}O record (dashed black line) and the normalized tuning target (gray line). Normalization followed standard techniques of subtracting the mean and dividing by the standard deviation. Panel b shows sedimentation rates based on obliquity derived age control points (see Table 2 in the EPSL Online Background Dataset[2]). Panels c, d, and e show a comparison of the filtered time series (solid black line in all panels represents δ^{18}O, black dashed line in panel c represents δ^{13}C) to the long and short eccentricity and lagged (7.2 ky) obliquity periods (gray lines), respectively. Panel f shows the inclination of the magnetization component for Site 1090 [11], placed on the orbitally tuned age model. Note that Site 1090 gives a Southern Hemisphere record; hence, negative inclination values represent normal polarity chrons as labeled. For a summary of the polarity chron boundaries, please refer to Table 1.

UNCORRECTED PROOF

ARTICLE IN PRESS

signal arises from local climatic processes on the adjacent continent (South America), which modulates the terrigenous input. The lag at the obliquity frequency presumably arises from the slow response of the Antarctic ice sheet.

Orbital tuning to lagged obliquity within the eccentricity weighted ETP yields very good agreement between the time series and the tuning target (Fig. 3). Although sedimentation rates vary by a factor of four to five over the entire time interval, across the Oligocene/Miocene boundary sedimentation, rates remain relatively constant at ~10 m/My (Fig. 3b). A comparison of the individual 400 ky (Fig. 3c) and 100 ky (Fig. 3d) eccentricity components yields a good match throughout the record (Fig. 3c and d), reflecting the overall quality of the tuned $\delta^{18}O$ record. The 100 ky filter output of the $\delta^{18}O$ data shows the 400 ky amplitude modulation of the eccentricity signal supporting the tuning strategy (Fig. 3d). There is only one exception, at ~21.0 Ma, where a high amplitude response of the filtered data exists due to sudden jumps in the original data that are most likely not real. At the obliquity scale, the match is very good only until ~18 Ma, after which it breaks down likely due to gaps in the record (Fig. 3e). Importantly, the obliquity component of the $\delta^{18}O$ record exhibits a 1.2 My amplitude modulation, which provides perhaps the most critical constraint on the tuned age model.

5. Time series analyses

We use the software package AnalySeries [18] to conduct the time series analysis. A Gaussian interpolation scheme is used to interpolate the data at the average 5 ky time step (interpolating across data gaps). After removing obvious outliers in the data (identified in Fig. 2a), we then filter the stable isotope records using band-pass Gaussian filters centered at 400, 100 and 40 ky periods to compare the geochemical variability with the corresponding orbital components of eccentricity and obliquity. We estimate power spectra, coherence and phase between the orbital target and the stable isotope records using the Blackman–Tukey method [19], as implemented in AnalySeries [18], with 247 lags (~15% of the series lengths) and an effective band width of ~1.5 My^{-1}.

Spectral and cross-spectral analyses verify the agreement between the orbital target and the $\delta^{18}O$ ($\delta^{13}C$) records (Fig. 4). The tuned $\delta^{18}O$ and $\delta^{13}C$ records contain significant concentration of variance and are coherent (above the 90 % significance level) at all orbital periods. They are coherent above the 99% significance level for long and short eccentricity, and main obliquity, for both isotope records (not shown). The climatic precession signal in the isotope data is relatively weak (e.g., Fig. 4a), and there are additional nonorbital peaks probably due to gaps in the stable isotope record. We also observe coherent power above the 90% significance level at ~54 and ~29 ky periods (components of obliquity) in both records. The ~29 ky peak is more significant (>95% significance, not shown) for the carbon isotope record. The $\delta^{18}O$ record is essentially in phase with the orbital target at all periods except at 96 ky (Fig. 4c). The in-phase relationship between the $\delta^{18}O$ record and the obliquity and precession periods demonstrates that the assumption of a 7.2 ky phase lag between obliquity and $\delta^{18}O$, which is adopted here based on retuning the Ceara Rise record to La_{2003}, is valid. The $\delta^{13}C$ record is not in phase with ETP at the eccentricity periods (Fig. 4d), but in phase at the obliquity and the climatic precession periods of 23 and 19 ky. Phase lags of $\delta^{13}C$ with respect to eccentricity (and hence $\delta^{18}O$, which is in phase with the longer eccentricity components) are not surprising; such temporal relationships may reflect the lagged response of the carbon cycle to climatic change [7].

6. Calibration of the GPTS

Magnetic measurements on Eocene to Miocene sediments from Site 1090 are described in detail by Channell et al. [11] who have augmented the shipboard paleomagnetic record with u-channel measurements as well as discrete (7 cm^3) samples. Aided by stable isotopic [11,14] and biostratigraphic [11,20–22] information, a polarity-zone pattern can be interpreted in terms of late Eocene through early Miocene polarity chrons [11]. GPTS ages in the Channell et al. [11] study are based on rescaling the ages of Cande and Kent [8,9] using the astronomically calibrated age of the O/M boundary of 22.9 Ma [10] as a revised calibration point. Note that our initial age model is

UNCORRECTED PROOF

ARTICLE IN PRESS

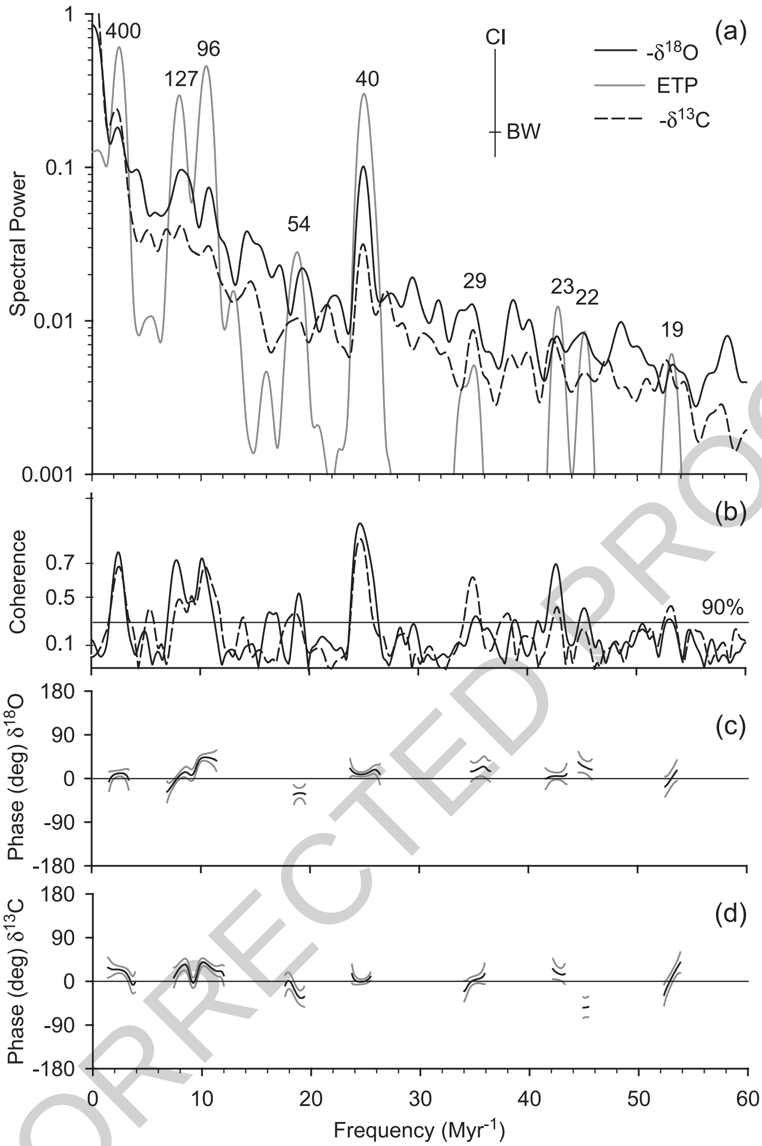

Fig. 4. Time series analyses of the Site 1090 benthic foraminiferal $\delta^{18}O$ and $\delta^{13}C$ records after tuning to obliquity. Spectral analyses were conducted using the AnalySeries [18] program (a), coherency (b) and $\delta^{18}O$ and $\delta^{13}C$ phase (c and d, respectively) estimates are based on Blackman–Tukey [19]. The 90% confidence interval and bandwidth are plotted in panel a. Note that positive phase angles indicate a lag of the $\delta^{18}O$ and $\delta^{13}C$ records with respect to the orbital target and that negative phase angles denote a lead (panels c and d, respectively).

UNCORRECTED PROOF

similar except we use a revised age of the O/M boundary, readjusted to the new astronomical model of Laskar et al. [12] of 23.0 Ma.

Orbital tuning of the Site 1090 $\delta^{18}O$ record to the ETP target curves provides astronomically tuned ages for late Oligocene through early Miocene polarity chrons (Fig. 3f, Table 1). With only one exception at the younger end of the record, the offset is less than one obliquity cycle between our initial age model and the final, astronomically tuned, time scale (Table 1). Tuning of the Site 1090 $\delta^{18}O$ record to obliquity scale yields particularly good results in two time slices: between ~18 and 20 Ma and between ~22 and 24 Ma (Figs. 5 and 6, respectively). Comparison of the

ARTICLE IN PRESS

Table 1
Summary of the revised ages for early Miocene through late Oligocene polarity chron boundaries

Chron	Site 1090 mcd (m)	Age (Ma) [8,9]	Revised spline age[a] (Ma) [8,9]	Site 1090 tuned age (Ma)	Offset: revised spline[a] and tuned age (Ma)
C5Cn.1n	71.40	16.014	15.914	15.898	0.016
C5Cn.1n	72.90	16.293	16.167	16.161	0.006
C5Cn.2n	73.50	16.327	16.197	16.255	– 0.058
C5Cn.2n	73.88	16.488	16.343	16.318	0.025
C5Cn.3n	74.40	16.556	16.404	16.405	0.000
C5Cn.3n	74.95	16.726	16.557	16.498	0.059
C5Dn	78.30	17.277	17.052	17.003	0.050
C5Dn	81.10	17.615	17.355	17.327	0.027
C5Dr.1r	82.28		17.530	17.511	0.020
C5Dr.1r	82.60		17.579	17.550	0.029
C5En	85.28	18.281	17.950	17.948	0.002
C5En	90.42	18.781	18.396	18.431	– 0.035
C6n	92.30	19.048	18.634	18.614	0.020
C6n	103.30	20.131	19.606	19.599	0.007
C6An.1n	106.77	20.518	19.955	19.908	0.047
C6An.1n	110.20	20.725	20.144	20.185	– 0.041
C6An.2n	112.30	20.996	20.390	20.420	– 0.030
C6An.2n	114.60	21.320	20.687	20.720	– 0.033
C6AAn	117.70	21.768	21.099	21.150	– 0.052
C6AAn	118.15	21.859	21.183	21.191	– 0.007
C6AAr.1n	120.80	22.151	21.455	21.457	– 0.002
C6AAr.1n	121.76	22.248	21.546	21.542	0.003
C6AAr.2n	123.80	22.459	21.743	21.737	0.006
C6AAr.2n	124.30	22.493	21.776	21.780	– 0.004
C6Bn.1n	125.10	22.588	21.865	21.847	0.019
C6Bn.1n	126.90	22.750	22.019	21.991	0.028
C6Bn.2n	127.35	22.804	22.070	22.034	0.036
C6Bn.2n	130.25	23.069	22.323	22.291	0.032
C6Cn.1n	134.65	23.353	22.596	22.593	0.003
C6Cn.1n	137.72	23.535	22.772	22.772	0.000
C6Cn.2n	140.50	23.677	22.911	22.931	– 0.020
C6Cn.2n	142.10	23.80	23.031	23.033	– 0.002
C6Cn.3n	145.90	23.999	23.228	23.237	– 0.009
C6Cn.3n	147.00	24.118	23.345	23.299	0.046
C7n.1n	158.75	24.730	23.959	23.988	– 0.029
C7n.1n	159.25	24.781	24.011	24.013	– 0.002
C7n.2n	160.35	24.835	24.066	24.138	– 0.072

[a] Provides the initial age model for Site 1090 based on a new age of the Oligocene/Miocene boundary of 23.0 Ma and recalculated spline ages of Cande and Kent [8,9].

obliquity filtered $\delta^{18}O$ record to lagged obliquity illustrates the close correlation of individual minima and maxima (Figs. 5a and 6a, top panels). The good match at the obliquity scale is clearly visible in the tuned $\delta^{18}O$ record (Figs. 5a and 6a, middle panels), where $\delta^{18}O$ minima coincide with obliquity maxima and vice versa. Figs. 5a and 6a also highlight the long-term eccentricity component contained in the $\delta^{18}O$ record; the most notable $\delta^{18}O$ maxima occur every ~400 ky during times of minimal eccentricity. Accordingly, early Miocene polarity chron C5En contains a minimum of 12 obliquity cycles, chron C6n contains 24.5 (Fig. 5c). Polarity chrons C6Cn.1n, C6Cn.2n and C6Cn.3n contain 4, 3 and 1.5 obliquity cycles, respectively (Fig. 6c), assuming that the record is complete. The comparison between the obliquity filtered $\delta^{13}C$ record and lagged obliquity exemplifies an in-phase behavior during the younger time interval

UNCORRECTED PROOF

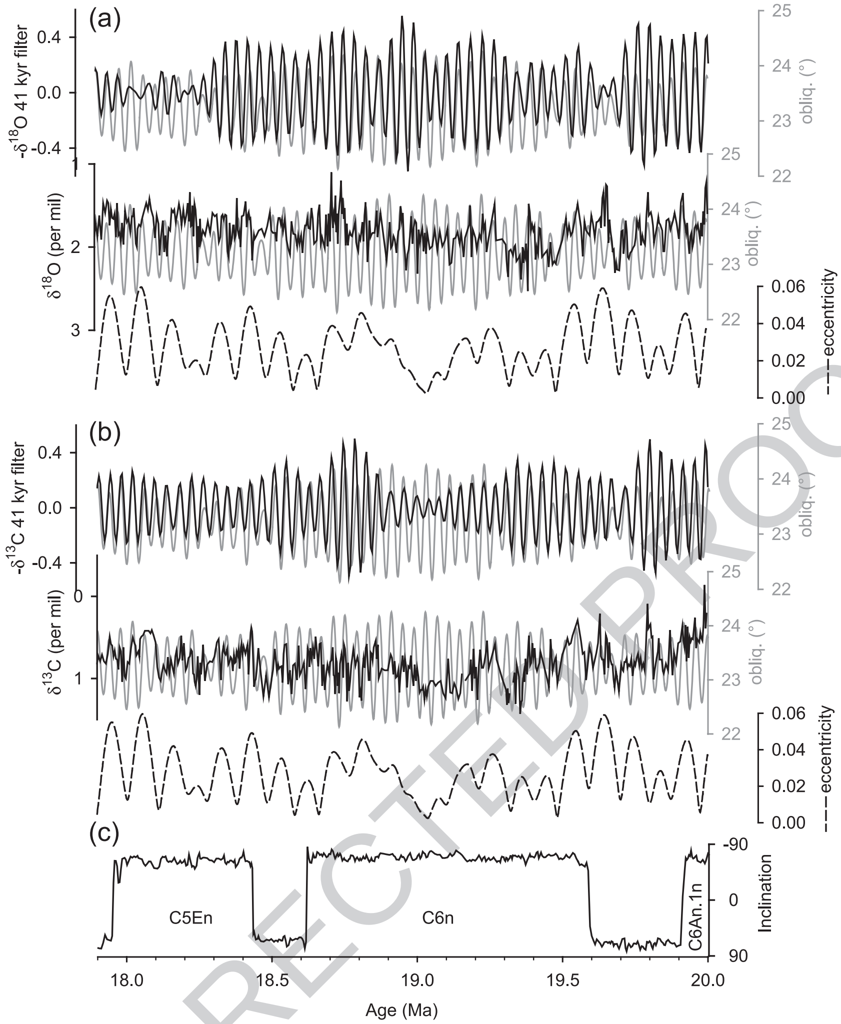

Fig. 5. Expanded early Miocene section (17.9–20.0 Ma) of the tuned oxygen (a), carbon (b), and the inclination of the magnetization component (c) records from Site 1090. In (a) and (b), the top panels illustrate the match between the lagged (7.2 ky) obliquity (gray line) and the 41 ky filter output of the tuned $\delta^{18}O$ ($\delta^{13}C$) record (black line). The middle panels compare the lagged (7.2 ky) obliquity (gray line) to the tuned $\delta^{18}O$ ($\delta^{13}C$) record. The bottom panels show variation in eccentricity (dashed black line). Early Miocene chron C5En contains a minimum of 12 obliquity cycles, chron C6n contains 24.5 assuming that the record is complete.

(Fig. 5b, top panel). However, during the older time slice, the two time series are in phase only until ~22.9 Ma (at ~22.9 Ma; Fig. 6b, top panel). As is the case for $\delta^{18}O$, long-term $\delta^{13}C$ variability is marked by prominent maxima following times of lowest eccentricity (Figs. 5b and 6b, bottom panel). As noted above, these observations agree with results from Ceara Rise and may indicate globally cooler climates associated with increased burial of organic carbon [7].

7. Discussion and conclusions

The Site 1090 benthic foraminiferal $\delta^{18}O$ record provides the first opportunity to directly calibrate a portion of the GPTS to astronomical models. Shackleton et al. [10] have already tuned a high-quality stable isotope record from Ceara Rise and, using the magnetostratigraphy of Holes 522 and 522A, refined the ages and duration of late Oligocene to earliest Miocene magnetochrons C7n through

UNCORRECTED PROOF

ARTICLE IN PRESS

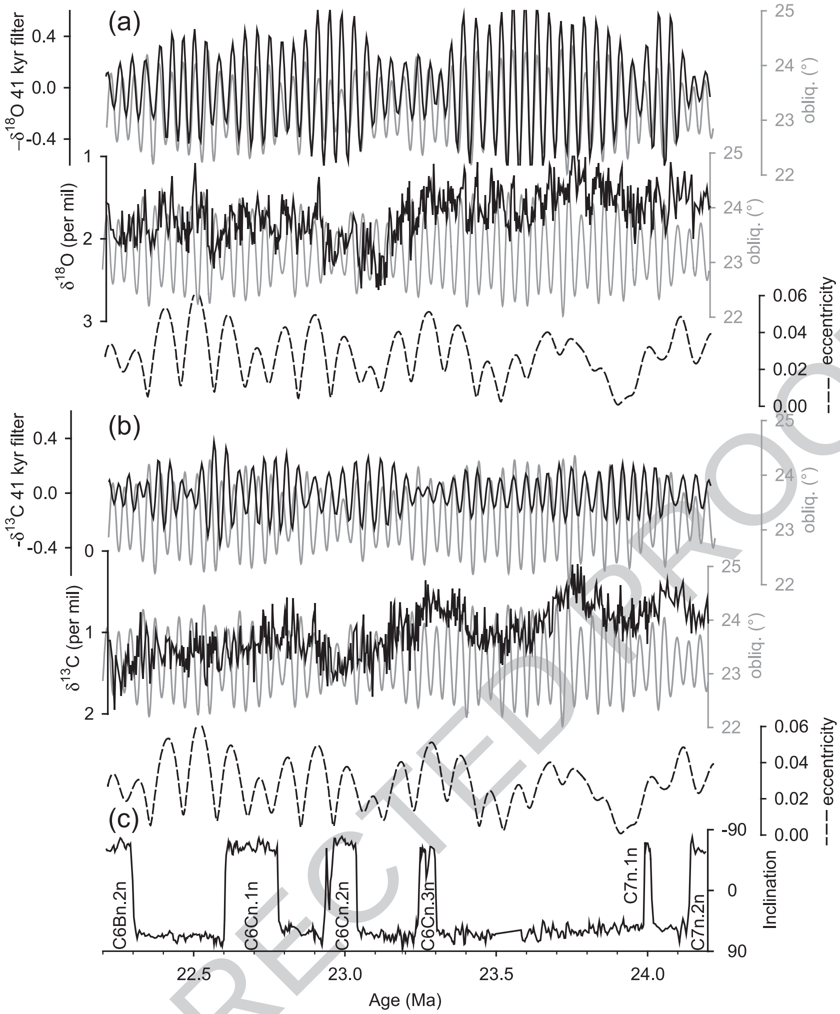

Fig. 6. Expanded late Oligocene/earliest Miocene section (22.2–24.2 Ma) of the tuned oxygen (a), carbon (b), and the inclination of the magnetization component (c) records from Site 1090. In (a) and (b), the top panels illustrate the match between the lagged (7.2 ky) obliquity (gray line) and the 41 ky filter output of the tuned $\delta^{18}O$ ($\delta^{13}C$) record (black line). The middle panels compare the lagged (7.2 ky) obliquity (gray line) to the tuned $\delta^{18}O$ ($\delta^{13}C$) record. The bottom panels show variation in eccentricity (dashed black line). Late Oligocene chrons C6Cn.1n, C6Cn.2n, and C6Cn.3n contain 4, 3, and 1.5 obliquity cycles, respectively, assuming that the record is complete.

C6Bn (21.9–24.07 Ma). The astronomical age calibration of Shackleton et al. [2,10] resulted in a revised, younger age for the Oligocene/Miocene boundary of ~23 Ma. Wilson et al. [23] questioned this revised age, and instead proposed an age of ~24 Ma, based on the chronostratigraphy of a drill core from the Ross Sea. Channell and Martin [24] have challenged these conclusions, and the 24 Ma age, based on ambiguities in the stratigraphy of this core.

Site 1090 supports the revised age of Shackleton et al [10]. For the interval where the Site 1090 record is least affected by gaps and outliers (~21–24 Ma, e.g., Fig. 2a), the amplitude variation of the $\delta^{18}O$ data at the obliquity scale suggest that they also follow the 1.2 Ma amplitude modulation pattern that is part of the astronomical solution. In particular, we can discern a successive pattern of high-, low- and high-amplitude 1.2 My cycles during this interval that are spaced at ~2.4 My intervals and which precludes the

UNCORRECTED PROOF

ARTICLE IN PRESS

age suggested by Wilson et al. [23] (Fig. 3e). We note that for this particular time interval, the succession of high and low 1.2 My amplitude nodes is similar for the astronomical solution used here [12] and a previous one [3]. Additionally, and independent of the detailed age model on the obliquity scale, we note the very close correspondence of the amplitudes between data and models at the 400 ky eccentricity time scale that also support our age model (Fig. 3c).

For early Miocene chrons C6AAr through C5Cn, the age model presented here is the first direct astrochronological calibration of the GPTS (Table 1). The rescaled ages derived from [8,9], using the latest O/M boundary age (23.0 Ma), are consistent with the final astronomically tuned age model for Site 1090 within one obliquity cycle with three exceptions: the end of C5Cn.2n, the onset of C5Cn.3n and the end of C5Dn, where age discrepancies are between 50 and 59 ky. As a result, our new age model supports not only the O/M boundary age (23.0 Ma) derived from Shackleton and others [10] but also both the relative duration of polarity chrons based on ocean magnetic anomaly data [8,9], and the middle Miocene calibration age (14.8 Ma for C5Bn) used by Cande and Kent [8,9] based on the correlation of the N9/N10 foraminiferal zonal boundary to the absolute ages of Tsuchi et al. [25] and Andreieff et al. [26]. It is the imprecise estimate of the O/M boundary age (23.8 Ma) used by Cande and Kent [8,9], derived from the chronogram ages for the stage boundary from Harland [27], that is the main source of error in the late Oligocene/early Miocene part of their time scale.

We conclude that obliquity tuning of the Site 1090 benthic foraminiferal $\delta^{18}O$ record enables us to refine the late Oligocene through early Miocene portion of the GPTS. Our statistical analyses, in particular, the 400 ky amplitude modulation of eccentricity and the 1.2 My modulation of obliquity, support our tuning strategy. Our results also provide independent evidence for a revised age of the Oligocene/Miocene boundary of 23.0 Ma.

Acknowledgements

We thank D. Kent, L. Lourens and an anonymous reviewer for helpful comments and suggestions that improved this publication. We also thank Mimi Katz for help with species identification. This research used samples provided by the Ocean Drilling Program (ODP). ODP is sponsored by the U.S. National Science Foundation (NSF) and participating countries under the management of Joint Oceanographic Institutions (JOI). This research was supported by NSF grant OCE 0095976 to K.B. and by NSF grant OCE 9711424 to J.C. and EAR 9725789 to J.Z. H.P. was supported by the Swedish Research Council (VR). Further support was provided by JOI/USSAP grants 177-F000784 to J.Z. and 177-F000785 to J.C. ***[EB]***

References

[1] N.J. Shackleton, S. Crowhurst, Sediment fluxes based on orbitally tuned time scale 5 Ma to 14 Ma, site 926, in: N.J. Shackelton, W.B. Curry, C. Richter, TJ. Bralower (Eds.), Proc. Ocean Drill. Prog., Sci. Results vol. 154, Ocean Drilling Program, College Station, TX, 1997, pp. 69–82.

[2] N.J. Shackleton, S.J. Crowhurst, G. Weedon, L. Laskar, Astronomical calibration of Oligocene–Miocene time, Philos. Trans. R. Soc. Lond. 357 (1999) 1909–1927.

[3] J. Laskar, F. Joutel, F. Boudin, Orbital, precessional, and insolation quantities for the Earth from −20 Ma to +10 Ma, Astron. Astrophys. 270 (1993) 522–533.

[4] J.C. Zachos, B.P. Flower, H. Paul, A high resolution chronology of orbitally paced climate oscillations across the Oligocene/Miocene boundary, Nature 388 (1997) 567–570.

[5] B.P. Flower, J.C. Zachos, E. Martin, Latest Oligocene through early Miocene isotopic stratigraphy and deep water paleoceanography of the western equatorial Atlantic: sites 926 and 929, in: N.J. Shackleton, W.B. Curry, C. Richter, T.J. Bralower (Eds.), Proc. Ocean Drill. Prog., Sci. Results vol. 154, Ocean Drilling Program, College Station, TX, 1997, pp. 451–464.

[6] H. Paul, J.C. Zachos, B.P. Flower, A. Tripati, Orbitally induced climate and geochemical variability across the Oligocene/Miocene boundary, Paleoceanography 15 (2000) 471–485.

[7] J.C. Zachos, N.J. Shackleton, J.S. Ravenaugh, H. Paelike, B.P. Flower, Climate response to orbital forcing across the Oligocene–Miocene boundary, Science 292 (2001) 274–278.

[8] S.C. Cande, D.V. Kent, A new geomagnetic polarity time scale for the late Cretaceous and Cenozoic, J. Geophys. Res. 97 (1992) 13917–13951.

[9] S.C. Cande, D.V. Kent, A new geomagnetic polarity time scale for the late Cretaceous and Cenozoic, J. Geophys. Res. 100 (1995) 6093–6095.

[10] N.J. Shackleton, M.A. Hall, I. Raffi, L. Tauxe, J. Zachos, Astronomical calibration age for the Oligocene–Miocene boundary, Geology 28 (2000) 447–450.

[11] J.E.T. Channell, S. Galeotti, E.E. Martin, K. Billups, H. Scher, J.S. Stoner, Eocene to Miocene magnetic, bio- and chemostratigraphy at ODP site 1090 (subantarctic South Atlantic), Geol. Soc. Amer. Bull. 115 (2003) 607–623.

UNCORRECTED PROOF

ARTICLE IN PRESS

[12] J. Laskar, M. Gastineau, F. Joutel, P. Robutel, B. Levrard, A., Correia, Long term evolution and chaotic diffusion of the insolation quantities of Mars, Icarus (in press).

[13] F. Varadi, B. Runnegar, M. Ghil, Successive refinements in long-term integrations of planetary orbits, Astrophys. J. 592 (2003) 620–630.

[14] K. Billups, J.E.T. Channell, J. Zachos, Late Oligocene to early Miocene geochronology and paleoceanography from the subantarctic South Atlantic, Paleoceanography 17 (2002) (10.1029/2000PA000568).

[15] M.E. Katz, D.R. Katz, L.D. Wright, G. Miller, D.K. Pak, N.J. Shackleton, E. Thomas, Early Cenozoic benthic foraminiferal isotopes: species reliability and interspecies correction factors, Paleoceanography 18 (2003) (doi: 10.1029/2002 PA000798).

[16] N.J. Shackleton, M. Hall, A. Boersma, Oxygen and carbon isotope data from Leg 74 foraminfers, Initial Rep. Deep Sea Drill. Proj. 74 (1984) 599–612.

[17] H. Pälike, J. Laskar, N.J. Shackleton, Geologic constraints on the chaotic diffusion of the Solar System, Geology (in review).

[18] D.L. Paillard, D.L. Labeyrie, P. Yiou, Macintosh program performs time-series analyses, Eos 77 (1996).

[19] G.M. Jenkins, D.G. Watts, Spectral Analysis and Its Applications, Holden-Day, Merrifield, VA, 1968.

[20] M. Marino, J.A. Flores, Miocene to Pliocene nannofossil biostratigraphy at ODP Leg 177 Sites 1088 and 1090, Mar. Micropaleontol. 45 (2002) 291–307.

[21] M. Marino, J.A. Flores, Middle Eocene to early Oligocene calcareous nannofossil stratigraphy at Leg 177 Site 1090, Mar. Micropaleontol. 45 (2002) 383–398.

[22] S. Garlotti, R. Coccioni, R. Gersonde, Middle Eocene–early Pliocene planktic foraminiferal biostratigraphy of ODP Leg 177, Site 1090, Agulhas Ridge, Mar. Micropaleontol. 45 (2002) 357–381.

[23] G.S. Wilson, M. Lavelle, W.C. McIntosh, A.P. Roberts, D.M. Harwood, D.K. Watkins, G. Villa, S.M. Bohaty, C.R. Fielding, F. Florindo, L. Sagnotti, T.R. Naish, R.P. Shere, K.L. Verosub, Integrated chronostratigraphic calibration of the Oligocene–Miocene boundary at 24 ± 0.1 Ma from the CRP-2A drill core, Ross Sea, Antarctica, Geology 30 (2002) 1043–1046.

[24] J.E.T. Channell, E.E. Martin, Comment on integrated chronostratigraphic calibration of the Oligocene–Miocene boundary at 24 ± 0.1 Ma from the CRP-2A drill core, Ross Sea, Antarctica, Geology, (2003) (doi: 10.1130/0091-7613).

[25] R. Tsuchi, Y. Takayanagi, K. Shibata, Neogene bioevents in the Japanese islands, in: R. Tsuchi (Ed.), Neogene of Japan—Its Biostratigraphy and Chronology, Kurofune Printing, Shizuoka, 1981, pp. 15–32.

[26] P. Andreieff, H. Bellon, D. Westercamp, Chronometrie et stratigraphie comparée des edifices volcaniques et formations sedimentaires de la Martinique (Antilles françaises), Bull. Bur. Rech. Geol. Min. 4 (1976) 335–346.

[27] W.B. Harland, R.L. Armstrong, A.V. Cox, L.E. Craig, A.G. Smith, D.G. Smith, A Geologic Time Scale, Cambridge Univ. Press, Cambridge, UK, (1990) 261 pp.

UNCORRECTED PROOF